

Stability and Causality in relativistic dissipative hydrodynamics

G. S. Denicol, T. Kodama, T. Koide and Ph. Mota

Instituto de Física, Universidade Federal do Rio de Janeiro, C. P. 68528, 21945-970, Rio de Janeiro, Brazil

The stability and causality of the Landau-Lifshitz theory and the Israel-Stewart type causal dissipative hydrodynamics are discussed. We show that the problem of acausality and instability are correlated in relativistic dissipative hydrodynamics and instability is induced by acausality. We further discuss the stability of the scaling solution. The scaling solution of the causal dissipative hydrodynamics can be unstable against inhomogeneous perturbations.

I. INTRODUCTION

Presently the hydrodynamical approach is known as one of basic tools for the description of the collective aspects of the relativistic heavy-ion collisions. However, instead of extensive analyses of experimental data based on this approach [1], the study of the effect of dissipation is yet poorly explored [2, 3, 4].

Till now, two basically different approaches to describe relativistic dissipative hydrodynamics are commonly employed; one is the relativistic extension of Navier-Stokes theory introduced by Landau-Lifshitz (LL) [5] and Eckart [6], and the other is the causal dissipative (CD) hydrodynamics or second order theory, where the version due to Israel-Stewart [7] is most popularly known. The relativistic Navier-Stokes theory (NS) is usually considered in the literature as a natural covariant generalization of the Navier-Stokes equation and in contrast to CD hydrodynamics, it is also referred to as the first order theory. Authors who apply the first order theory argue that the second order theory is not yet completely established and the difference of two approaches would be not significant, since the effect of viscosity is the measure of the deviation from the local thermodynamical equilibrium, and should be small where the hydrodynamical approach is meaningful. However, a crucial point of the reason why the second order approach should be explored is that the propagation speed in the first order theory is infinite and it does not satisfy the relativistic causality. It is also known that the first order theory leads to dynamical instabilities. These aspects are not only the question of conceptions but also related to serious practical problems and deserve a more detailed analysis.

One way to solve the problem of acausality in a first order theory is to introduce, for example, a memory effect with a finite relaxation time [3]. In this way, we can derive a CD hydrodynamics from the LL theory. There are several different approaches to derive the CD hydrodynamics [3, 7, 8, 9, 10, 11]. In this work, we consider the Israel-Stewart type CD hydrodynamics.

A crucial point is whether a relativistic dissipative hydrodynamics is stable or not. If a theory is unstable, it will be very difficult to extract any physically meaningful results from it. The analysis of the stability of relativistic dissipative hydrodynamics has been extensively studied by Hiscock and his collaborators [12, 13, 14, 15, 16, 17]. Their conclusions are summarized as follows. 1) The Eckart theory is unstable for the linear perturbation around the hydrostatic states whereas the LL theory and the IS theory (of the Landau frame) are stable [13, 14]. 2) The LL theory is shown to be unstable for the linear perturbation around hydrostatic states in a general frame where the fluid is Lorentz boosted [13].

Another important analysis was implemented by Kouno et al [18]. They discussed the linear perturbation around the scaling solution of the LL theory and found that the scaling solution of the LL theory can be unstable. A similar discussion is repeated by [19] using another equation of state.

The purpose of this paper is to complement these discussions. We will, in particular, focus on two subjects. One is the relation between causality and stability. In general, the concept of causality and stability are independent, but in relativistic systems, as we will see, they are closely related. To show this, we discuss the stability from Lorentz boosted frames and show that instability is induced because of acausality.

The other is the stability around the scaling solution in the CD hydrodynamics. In the LL theory, the scaling solution can be unstable, although it is always stable when the Reynolds number is larger than one. The stability around the scaling solution has not yet been discussed in the CD hydrodynamics. The applicability of the scaling ansatz is not obvious in the CD hydrodynamics, because, as we will see later, the numerical calculation of the CD hydrodynamics shows a kind of non-periodic oscillations in the central rapidity region.

In this paper, we restrict ourselves to the discussion on 1+1 dimensional motion of massless ideal gas (to be specific, an ideal three flavor massless QGP gas), for simplicity. This paper is organized as follows. In section II, we discuss the stability and causality around the hydrostatic states. The result of this section has already been shown in [4, 13, 14]. To establish the relation between causality and stability, we discuss the stability of the hydrostatic state from Lorentz boosted frames in section III. In section IV, the stability around the scaling solution is discussed. Section V is devoted to concluding remarks.

II. LINEAR PERTURBATION AROUND THE HYDROSTATIC STATE

Before discussing the relation between causality and stability, we will discuss first the stability near the hydrostatic state following [4, 13, 14].

In the CD hydrodynamics of 1+1 dimensional systems, the equations are given by

$$\partial_\nu T^{\mu\nu} = 0, \quad (1)$$

$$\tau_R \frac{d}{d\tau} \Pi + \Pi = -\zeta \partial_\mu u^\mu. \quad (2)$$

Here, Π is the bulk viscosity and $T^{\mu\nu}$ is the energy-momentum tensor defined by

$$T^{\mu\nu} = (\varepsilon + P + \Pi)u^\mu u^\nu - (P + \Pi)g^{\mu\nu}, \quad (3)$$

where ε , P and u^μ are the energy density, pressure and four-velocity of the fluid, respectively. For the massless QGP, we have $\varepsilon = 3P$, and $\varepsilon + P = Ts$, where T and s are the temperature and entropy density, respectively. The fluid velocity is determined from the energy-momentum tensor following the definition of Landau-Lifshitz [5]. It should be noted that the CD hydrodynamics is reduced to the LL theory in the limit of the vanishing relaxation time τ_R .

For later convenience, we parametrize the velocity as follows,

$$u^\mu = (\cosh \theta, \sinh \theta). \quad (4)$$

We adopt the following parametrization of the bulk viscosity coefficient and the relaxation time [4],

$$\zeta = as, \quad (5)$$

$$\tau_R = \frac{\zeta}{\varepsilon + P} b, \quad (6)$$

where s is the entropy density. The parameters a and b characterize respectively the magnitudes of the viscosity and the relaxation time [20]. As we will see later, the parameter b should be smaller than 3/2 to be consistent with causality [3].

We consider the plane wave perturbation around ε_0 , θ_0 and Π_0 ,

$$\varepsilon(t, x) \approx \varepsilon_0(t, x) + \epsilon \varepsilon_1(t, x), \quad (7)$$

$$\theta(t, x) \approx \theta_0(t, x) + \epsilon \theta_1(t, x), \quad (8)$$

$$\Pi(t, x) \approx \Pi_0(t, x) + \epsilon \Pi_1(t, x), \quad (9)$$

with

$$\begin{pmatrix} \varepsilon_1(t, x) \\ \theta_1(t, x) \\ \Pi_1(t, x) \end{pmatrix} = e^{i\omega t - ikx} \begin{pmatrix} \varepsilon_1 \\ \theta_1 \\ \Pi_1 \end{pmatrix}. \quad (10)$$

Here ϵ is a small expansion parameter. The two transport coefficients are also expanded as

$$\zeta \approx \zeta_0 + \epsilon \delta \zeta, \quad (11)$$

$$\tau_R \approx \tau_{R0} + \epsilon \delta \tau_R. \quad (12)$$

For the linear perturbation around the hydrostatic state,

$$\varepsilon_0 = \text{const}, \quad \theta_0 = \Pi_0 = 0, \quad (13)$$

the evolution equation of the linear perturbation is given by

$$A \begin{pmatrix} \varepsilon_1 \\ \theta_1 \\ \Pi_1 \end{pmatrix} = 0, \quad (14)$$

where

$$A = \begin{pmatrix} i\omega & -ik(\varepsilon_0 + P_0) & 0 \\ \alpha(-ik) & i\omega(\varepsilon_0 + P_0) & -ik \\ 0 & -ik\zeta_0 & 1 + \tau_{R0}i\omega \end{pmatrix}, \quad (15)$$

where $\alpha = \partial P/\partial \varepsilon = 1/3$. To have non-trivial solutions, the determinant of the matrix A should vanish so that the frequency ω has to satisfy the following dispersion relation,

$$\omega^3 - \frac{i}{\tau_{R0}}\omega^2 - \left(\frac{\zeta_0}{\tau_R} \frac{1}{\varepsilon_0 + P_0} + \alpha \right) k^2 \omega + i \frac{\alpha}{\tau_{R0}} k^2 = 0. \quad (16)$$

The behaviors of the frequency characterizes the stability and the propagation speed of the fluid.

A. Landau-Lifshitz theory

We consider the case of the LL theory by taking $\tau_R = 0$. Then the solution of the dispersion relation (16) is analytically given by

$$\omega = \frac{i\zeta_0}{2(\varepsilon_0 + P_0)} \pm \sqrt{\alpha k^2 - \frac{\zeta_0^2}{4(\varepsilon_0 + P_0)^2} k^4}. \quad (17)$$

The real and imaginary parts of the frequency ω are shown in Fig. 1 for $a = 0.1$ and $T = 200$ MeV, respectively. One can easily see that the behavior of ω changes at the critical momentum $k_c = 2\sqrt{\alpha}(\varepsilon_0 + P_0)/\zeta_0$; below the critical momentum, there are two propagating modes, while they are changed to two non-propagating modes above it.

We assume that the propagation speed of fluid is characterized by the group velocity for propagating modes. Then, the causality of the theory is determined by the behavior of the real parts of the frequencies. For the small k , the propagation speed is given by

$$v = \frac{\partial \text{Re } \omega}{\partial k} \approx \sqrt{\alpha}. \quad (18)$$

This is nothing but the usual sound velocity, and the LL theory seems to be consistent with causality. For the large k , however, the propagating modes are changed to the non-propagating modes which show k^2 dependence. This momentum dependence is the same behavior as that of the non-propagating mode in diffusion processes, where the propagation speed is infinite. It is considered that the behavior of the non-propagating mode is the origin of acausality in the LL theory.

On the other hand, the stability of the theory is characterized by the behaviors of the imaginary parts of the frequencies. One can easily see that the two modes always have positive imaginary parts, and hence the LL theory is stable under the linear perturbation around the hydrostatic states.

Note that this is different behavior from the Eckart theory, where the theory is acausal and unstable even for the linear perturbation around the hydrostatic state [13].

B. Causal dissipative hydrodynamics

Different from the case of the LL theory, we can still obtain the dispersion relation from Eq.(16), but the analytic form of the solution becomes extremely complicated. However, in the large k limit, we have [4]

$$\omega = \begin{cases} \pm k \sqrt{\frac{1}{b} + \alpha + \frac{i}{2\tau_R(1+\alpha b)}} , \\ i \frac{\alpha b}{\tau_R(1+\alpha b)} \end{cases}, \quad (19)$$

while for the small k ,

$$\omega = \begin{cases} \pm k \frac{\sqrt{\alpha - (\alpha + 1/(4b))\tau_R^2 k^2/b}}{1 - \tau_R^2 k^2/b} + \frac{ik^2 \tau_R}{2(b - \tau_R^2 k^2)} . \\ i/\tau_R \end{cases}. \quad (20)$$

In this case, there are three modes; two of them are propagating modes and the remaining one is a non-propagating mode. From Eqs.(19) and (20), we can see that, for the small k , the group velocity of the propagating modes reduces to that of the ideal one, $\sqrt{\alpha}$, like the LL theory. On the other hand, for the large k , the group velocity is given by

$$v_c = \sqrt{1/b + \alpha}. \quad (21)$$

That is, the group velocity is affected by the bulk viscosity. This gives the maximum propagation speed of this fluid.

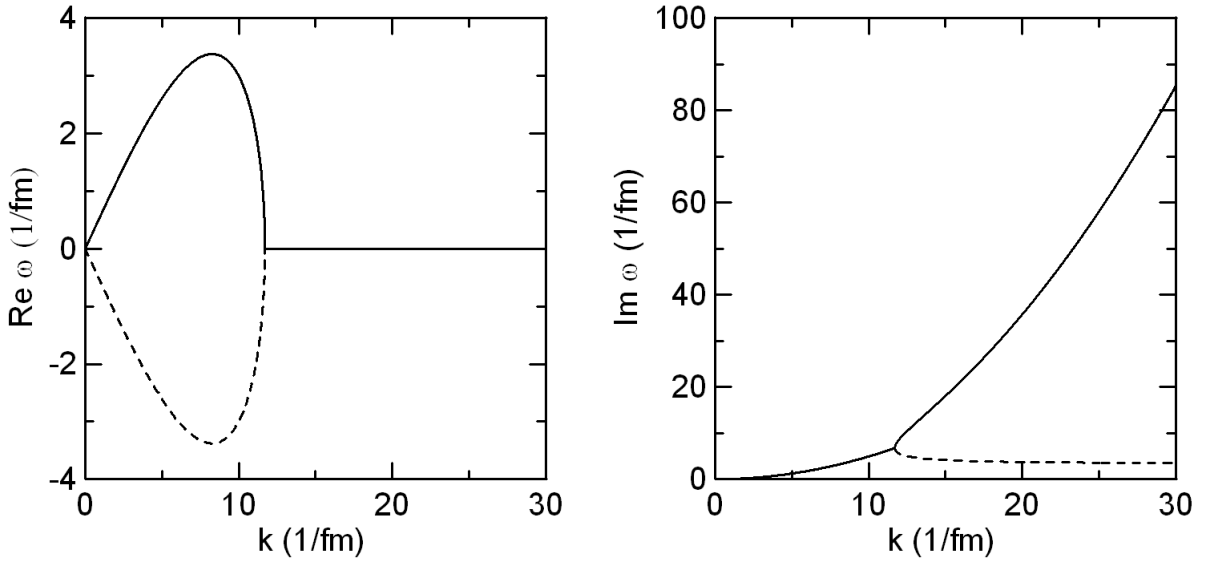


FIG. 1: The real (left panel) and imaginary (right panel) parts of the frequency in the Landau-Lifshitz theory at the rest frame. The two propagating modes (the solid and dotted lines) are changed to the non-propagating modes at the critical k_c . Both of them have positive values.

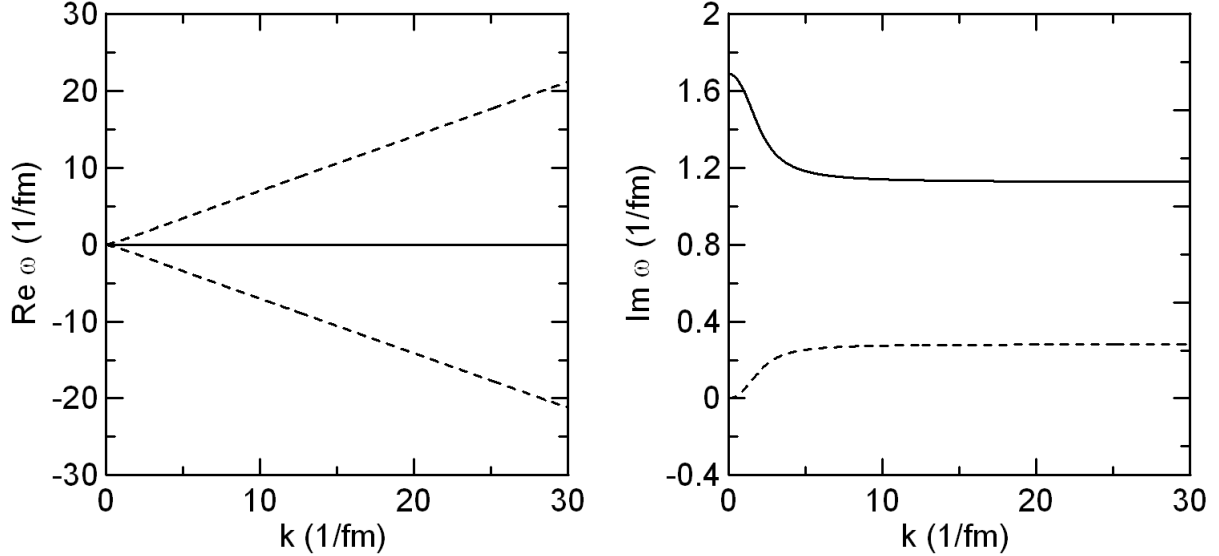


FIG. 2: The real (left panel) and imaginary (right panel) parts of the frequency in the causal dissipative hydrodynamics at the rest frame for $a = 0.1$ and $b = 6$. There are three modes. One is non-propagating mode (the solid line), and the other two are propagating modes (the dotted lines). The two imaginary parts of the propagating modes are degenerated.

In Fig. 2, we show the real and imaginary parts of the frequency ω as functions of momentum k for $a = 0.1$, $b = 6$, and the temperature $T = 200 \text{ MeV}$. From the left panel, one can see that the group velocity of the two propagating modes $\partial \text{Re } \omega / \partial k$ are still slower than the speed of light. As for the non-propagating mode, we find, from the right panel, that the imaginary part becomes a constant for the large k , always remaining positive. This is true for the two propagating modes. The positivity of the imaginary part guarantees the stability of the hydrostatic state for plane-wave perturbations. That is, the CD hydrodynamics, with this parameter set, is causal and stable.

However, as was mentioned, the propagation speed of the fluid (21) is affected by the parameter b . For the ideal equation of state, $\alpha = 1/3$, the propagation speed exceeds the speed of light if we use the parameter $b < 3/2$. In Fig. 3, the real and imaginary parts of ω as functions of momentum k are plotted for $a = 0.1$, $b = 1$, and the temperature $T = 200 \text{ MeV}$. In this acausal parameter set, v_c is larger than one, and hence, as one can see from the left panel, the propagation speed of the propagating modes $\partial \text{Re } \omega / \partial k$ exceeds the speed of light. That is, *even the*

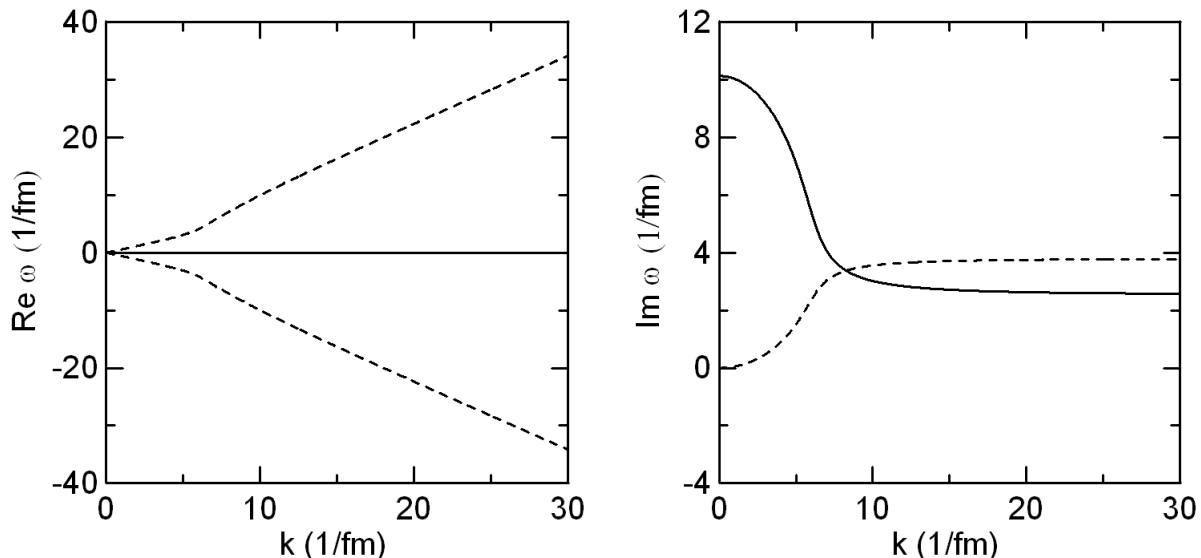


FIG. 3: The real (left panel) and imaginary (right panel) parts of the frequency in the causal dissipative hydrodynamics at the rest frame for $a = 0.1$ and $b = 1$. There are three modes. One is non-propagating mode (the solid line), and the other two are propagating modes (the dotted lines). The two imaginary parts of the propagating modes are degenerated.

CD hydrodynamics can be acausal depending on parameter sets. However, all the modes have negative imaginary parts and the theory is still stable.

From these results, one may consider that the problem of acausality is independent of that of instability. However, as we will see in the next section, both problems are correlated in relativistic systems.

In this section, we discussed the propagation speed under the linear approximation. It should be noted that the propagation speed is changed when the non-linear effect is taken into account. See Appendix A for details.

III. STABILITY IN GENERAL EQUILIBRIUM FRAME

In the previous section, we discussed the stability of a small perturbation mode around the hydrostatic state. Then we found that even if the dynamics is not consistent with causality (the LL theory and the CD hydrodynamics with the acausal parameter set), the hydrostatic states are still stable. Thus stability is not related with the causality of the theory in these mode. However, these two should be related. Suppose an acausal propagation of a wave in a covariant theory is allowed. Then an initial pulse within the light-cone eventually would develop a singular behavior at the light-cone, since the light-cone cannot be crossed within a covariant theory. To clarify this point, we will investigate the behaviors of the perturbation in a general Lorentz boosted frame.

Let us consider the linear perturbation around the hydrostatic state from the Lorentz boosted frame moving with the velocity V . Then the total velocity of the fluid is given by

$$\begin{aligned} U^{\mu'} &= \gamma_V (\cosh \theta + V \sinh \theta, V \cosh \theta + \sinh \theta), \\ &= \cosh(\psi + \theta) (1, \tanh(\psi + \theta)), \end{aligned} \quad (22)$$

where $\tanh \psi = V$.

Substituting this into the energy-momentum tensor and repeating the same linear analysis around the hydrostatic state with ψ being maintained constant, the evolution equation for the linear perturbation is given by

$$A \begin{pmatrix} \varepsilon_1 \\ \theta_1 \\ \Pi_1 \end{pmatrix} = 0, \quad (23)$$

where the components of the matrix are

$$A_{11} = (\cosh^2 \psi + \sinh^2 \psi \alpha)(i\omega) + \cosh \psi \sinh \psi (1 + \alpha)(-ik), \quad (24)$$

$$A_{12} = 2(\varepsilon_0 + P_0) \cosh \psi \sinh \psi (i\omega) + w_0(\cosh^2 \psi + \sinh^2 \psi)(-ik), \quad (25)$$

$$A_{13} = \sinh^2 \psi (i\omega) + \cosh \psi \sinh \psi (-ik), \quad (26)$$

$$A_{21} = \cosh \psi \sinh \psi (1 + \alpha)(i\omega) + (\sinh^2 \psi + \cosh^2 \psi \alpha)(-ik), \quad (27)$$

$$A_{22} = w_0(\cosh^2 \psi + \sinh^2 \psi)(i\omega) + 2w_0 \cosh \psi \sinh \psi (-ik), \quad (28)$$

$$A_{23} = \cosh \psi \sinh \psi (i\omega) + \cosh^2 \psi (-ik), \quad (29)$$

$$A_{31} = 0, \quad (30)$$

$$A_{32} = \zeta_0(\sinh \psi (i\omega) + \cosh \psi (-ik)), \quad (31)$$

$$A_{33} = \tau_{R0} \cosh \psi (i\omega) + \tau_{R0} \sinh \psi (-ik) + 1. \quad (32)$$

Then the dispersion relation is obtained by solving the following equation,

$$iA\omega^3 + iBk\omega^2 + C\omega^2 + iDk^2\omega + Ek\omega + iFk^3 + Gk^2 = 0, \quad (33)$$

where

$$A = \cosh \theta(-1 - (1 - v_c^2) \sinh^2 \psi), \quad (34)$$

$$B = \sinh \psi(1 - (1 - v_c^2) + 3(1 - v_c^2) \cosh^2 \psi), \quad (35)$$

$$C = -\frac{1}{\tau_{R0}}(\alpha + (1 - \alpha) \cosh^2 \psi), \quad (36)$$

$$D = \cosh \psi(-3(1 - v_c^2) \cosh^2 \psi + 2(1 - v_c^2) + 1), \quad (37)$$

$$E = \frac{2}{\tau_{R0}}(1 - \alpha) \cosh \psi \sinh \psi, \quad (38)$$

$$F = \sinh \psi(-1 + (1 - v_c^2) \cosh^2 \psi), \quad (39)$$

$$G = \frac{1}{\tau_{R0}}(1 - (1 - \alpha) \cosh^2 \psi). \quad (40)$$

One can easily see that the behavior of the frequency ω depends on the choice of v_c , which is the propagation speed of the fluid defined by Eq. (21).

A. Landau-Lifshitz theory

As we discussed, the Landau-Lifshitz theory has two modes in the local rest frame. In the Lorentz boosted frame, however, we have three modes, because of the following reason. In this case, the coefficients of Eq. (33) are given by;

$$A = \zeta_0 \cosh \psi \sinh^2 \psi, \quad (41)$$

$$B = \zeta_0 \sinh \psi(1 - 3 \cosh^2 \psi), \quad (42)$$

$$C = -(\varepsilon_0 + P_0)(\alpha + (1 - \alpha) \cosh^2 \psi), \quad (43)$$

$$D = \zeta_0 \cosh \psi(-2 + 3 \cosh^2 \psi), \quad (44)$$

$$E = 2(\varepsilon_0 + P_0)(1 - \alpha) \cosh \psi \sinh \psi, \quad (45)$$

$$F = -\zeta_0 \sinh \psi \cosh^2 \psi, \quad (46)$$

$$G = (\varepsilon_0 + P_0)(1 - (1 - \alpha) \cosh^2 \psi). \quad (47)$$

The coefficient A disappears only in the rest frame ($\psi = 0$). That is, there exists a gap in the calculations of the rest frame and the moving frame.

In Fig. 4, the real and imaginary parts of the frequency ω are shown for $a = 0.1$ and $T = 200$ MeV at $V = 0.1$. One can see that all the three modes are propagating modes. The real parts of the two propagating modes denoted by the dotted line are degenerated, but the imaginary part of one of them is negative. Thus the LL theory is unstable in the Lorentz boosted frame.

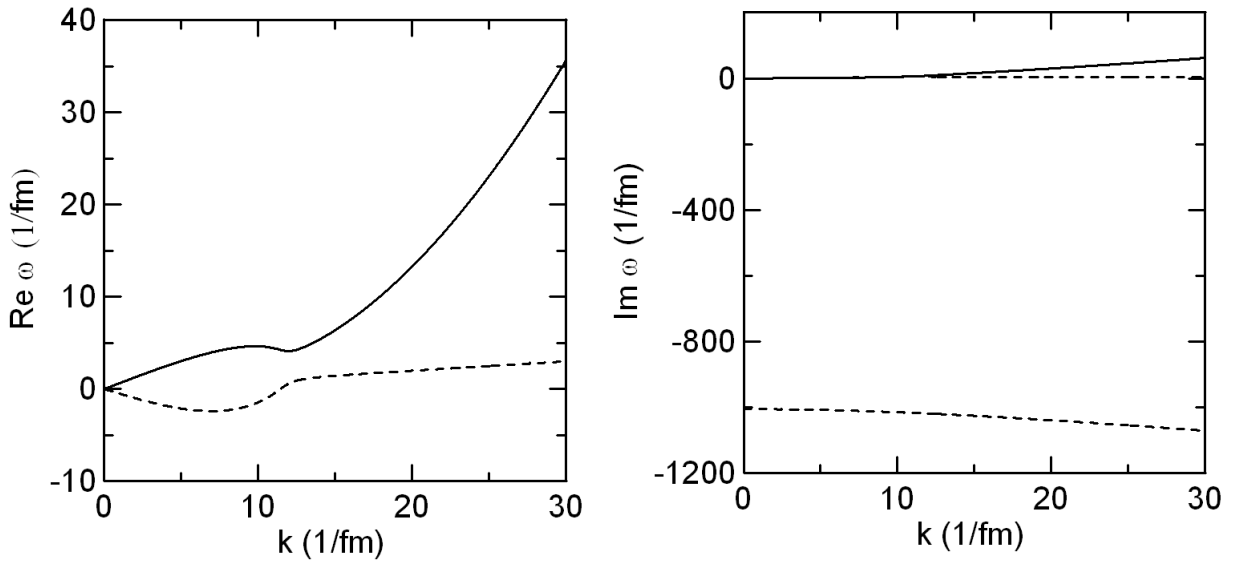


FIG. 4: The real (left panel) and imaginary (right panel) parts of the frequency in the Landau-Lifshitz theory in the Lorentz boosted frame with the velocity $v = 0.1$. There are three propagating modes. One of the modes is denoted by the solid line. The remaining two modes are degenerated and plotted by the dotted line. One of the imaginary parts (one of the dotted lines) is negative.

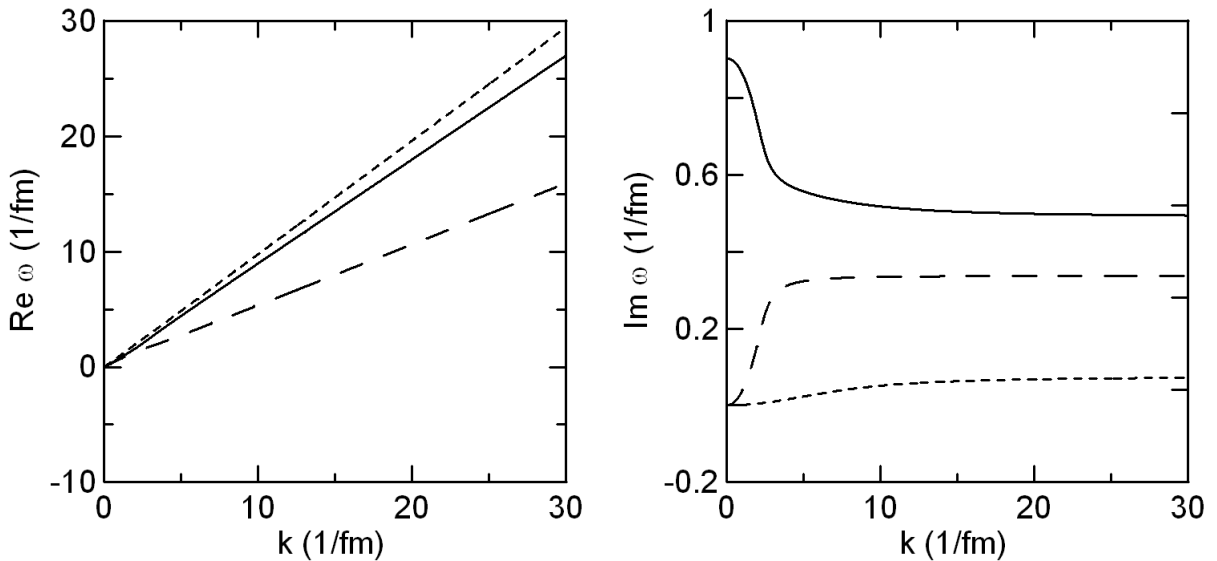


FIG. 5: The real (left panel) and imaginary (right panel) parts of the frequency in the causal dissipative hydrodynamics in the Lorentz boosted frame with the velocity $v = 0.9$ for $a = 0.1$ and $b = 1$. There are three modes denoted by the solid, dotted and dashed lines, respectively. All modes have positive imaginary parts.

B. Causal dissipative hydrodynamics

First, we consider the causal parameter set, $a = 0.1$ and $b = 6$ where the propagation speed (21) is slower than the speed of light. In Fig. 5, the real and imaginary parts of the frequency ω are shown for $T = 200$ MeV at $V = 0.9$. From the behaviors of the real parts, one can see that the three group velocities become close to the speed of light, but never exceed. On the other hand, all three propagating modes have positive imaginary parts. As far as we checked, this theory does not become acausal and does not have a negative imaginary part for any V . Thus in this causal parameter set, the CD hydrodynamics is consistent with causality and stable even in the Lorentz boosted frame.

However, this is not true for the acausal parameter set, for example, $a = 0.1$ and $b = 1$. In Fig. 6, we show the real and imaginary parts of the frequency ω . There are three propagating modes denoted by the solid, dashed and dotted

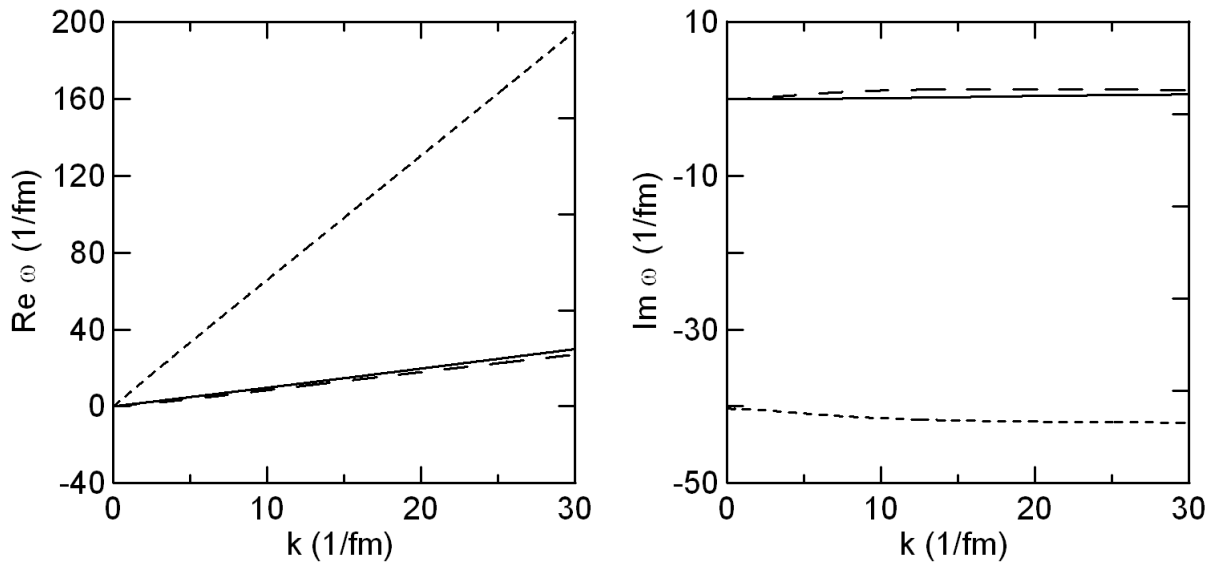


FIG. 6: The real (left panel) and imaginary (right panel) parts of the frequency in the causal dissipative hydrodynamics in the Lorentz boosted frame with the velocity $v = 0.9$ for $a = 1$ and $b = 1$. There are three modes denoted by the solid, dotted and dashed lines, respectively. One mode (the dotted line) has a negative imaginary part.

line. It is clear that the group velocity is faster than the speed of light. Interestingly enough, one of the propagating modes denoted by the dotted line has a negative imaginary part. Thus the CD hydrodynamics with acausal parameter set is unstable in the Lorentz boosted frame.

This result means that causality and stability are correlated and instability is induced by acausality in the relativistic dissipative hydrodynamics. A consistent theory should not change its stability depending on the choice of the frames. Thus, the LL theory is not consistent theories as candidates for the relativistic dissipative hydrodynamics. This is so also for the CD hydrodynamics with acausal parameter sets.

We should stress, as a matter of fact, that we cannot implement stable numerical calculations of the CD hydrodynamics when we use acausal parameter sets.

The stability of the LL theory from a general frame is discussed also in [13] in a different context. See Appendix B for details.

IV. STABILITY AROUND SCALING SOLUTION

In this section, we discuss the stability around the scaling solution. The scaling variables τ and y are defined by

$$\tau = \sqrt{t^2 - z^2}, \quad y = \frac{1}{2} \ln \left[\frac{t+z}{t-z} \right]. \quad (48)$$

By using these variables, the equations for the conservation of energy-momentum are reexpressed as

$$(\tau \partial_\tau + \tanh(\theta - y \pm \theta_s) \partial_y)(\phi \pm \theta) - \frac{\tau}{\cosh(\theta - y) \pm c_s \sinh(\theta - y)} R^{-1} \left[c_s \nabla \theta \pm \left(D\theta + \frac{1}{\Pi} \nabla \Pi \right) \right] = 0, \quad (49)$$

where $\tanh \theta_s = \sqrt{\alpha}$. Here we define the Reynolds number $R^{-1} = -\Pi/(Ts)$, which reproduces the definition of [18] in the vanishing relaxation time limit. The new variable ϕ satisfies the following relation,

$$d\phi = \sqrt{\alpha} d \ln s = \frac{1}{\sqrt{\alpha}} d \ln T. \quad (50)$$

The equation for the viscosity is

$$\tau_R \partial_\tau \Pi + \Pi = -\zeta \left(\sinh(\theta - y) \partial_\tau + \cosh(\theta - y) \frac{1}{\tau} \partial_y \right) \theta. \quad (51)$$

We assume that the velocity of the fluid is given by

$$\tanh \theta = \frac{z}{t} = \tanh y. \quad (52)$$

This scaling ansatz is considered to be valid near the central rapidity region. Thus, the equations of the scaling solution are given by setting $\theta = y$,

$$\tau \partial_\tau \phi_0 + (1 - R_0^{-1}) c_s^0 = 0, \quad (53)$$

$$\tau_{R0} \partial_\tau \Pi_0 + \Pi_0 = -\frac{\zeta_0}{\tau}. \quad (54)$$

In the LL limit ($\tau_R \rightarrow 0$), the equations are reduced to those obtained in [18].

To see the stability of the scaling solution, we consider the linear perturbation as follows,

$$\theta = y + \delta\theta, \quad (55)$$

$$\phi = \phi_0 + \delta\phi. \quad (56)$$

Substituting them into Eqs. (49) and (51), the evolution equations of the linear perturbations are given by

$$\tau \partial_\tau \delta\phi + (1 - R_0^{-1}) c_s^0 \partial_y \delta\theta + (1 - R_0^{-1}) \left(\frac{\partial c_s}{\partial \phi} \right)_0 \delta\phi - \delta R^{-1} c_s^0 = 0, \quad (57)$$

$$\tau (1 - R_0^{-1}) \partial_\tau \delta\theta + c_s^0 \partial_y \delta\phi + (1 - (c_s^0)^2) \delta\theta - (1 - (c_s^0)^2) \delta\theta R_0^{-1} - \frac{R_0^{-1}}{\Pi_0} \partial_y \delta\Pi + \frac{1}{\Pi_0} \frac{R_0^{-1}}{\tau_R} (\tau \Pi_0 + \zeta_0) \delta\theta = 0, \quad (58)$$

$$\tau_{R0} \partial_\tau \delta\Pi + \delta\Pi = \left(\frac{\partial \ln \tau_R}{\partial \phi} \right)_0 (\Pi_0 + \frac{\zeta_0}{\tau}) \delta\phi - \frac{\zeta_0}{\tau} \left(\frac{\partial \ln \zeta}{\partial \phi} \right)_0 \delta\phi - \zeta_0 \frac{\partial_y \delta\theta}{\tau}, \quad (59)$$

where

$$\delta R^{-1} = -\frac{1}{(Ts)_0} \delta\Pi + \frac{\Pi_0}{(Ts)_0} \left(\frac{\partial \ln(Ts)}{\partial \phi} \right)_0 \delta\phi, \quad (60)$$

with the scaling solutions ϕ_0 and Π_0 .

By using the Fourier transform for y ,

$$A(\tau, y) = \int dk e^{-iky} A(\tau, k), \quad (61)$$

Eqs. (57), (58) and (59) are summarized as

$$\tau \partial_\tau X = AX, \quad (62)$$

where

$$X = \begin{pmatrix} \delta\phi \\ \delta\theta \\ \delta \ln \Pi \end{pmatrix}, \quad (63)$$

and

$$A = \begin{pmatrix} -(1 - R_0^{-1}) \left(\frac{\partial \sqrt{\alpha}}{\partial \phi} \right)_0 - R_0^{-1} (1 + \alpha) & -(1 - R_0^{-1}) \sqrt{\alpha} (-ik) & \sqrt{\alpha} R_0^{-1} \\ -\sqrt{\alpha} \frac{(-ik)}{(1 - R_0^{-1})} & -(1 - \alpha) - \frac{(R_0^{-1} \hat{\tau} - \frac{1}{b})}{(1 - R_0^{-1})} & R_0^{-1} \frac{(-ik)}{(1 - R_0^{-1})} \\ -\sqrt{\alpha} \left(\hat{\tau} - \frac{1}{R_0^{-1} b} \right) + \frac{1}{\sqrt{\alpha} R_0^{-1} b} & \frac{-ik}{R_0^{-1} b} & -\frac{1}{R_0^{-1} b} \end{pmatrix}, \quad (64)$$

where $\hat{\tau} = \tau/\tau_{R0}$ and

$$\frac{\partial \ln(Ts)}{\partial \phi} = \sqrt{\alpha} + \frac{1}{\sqrt{\alpha}}, \quad (65)$$

$$\frac{\partial \ln \tau_{R0}}{\partial \phi} = -\sqrt{\alpha}, \quad (66)$$

$$\frac{\partial \ln \zeta}{\partial \phi} = \frac{1}{\sqrt{\alpha}}. \quad (67)$$

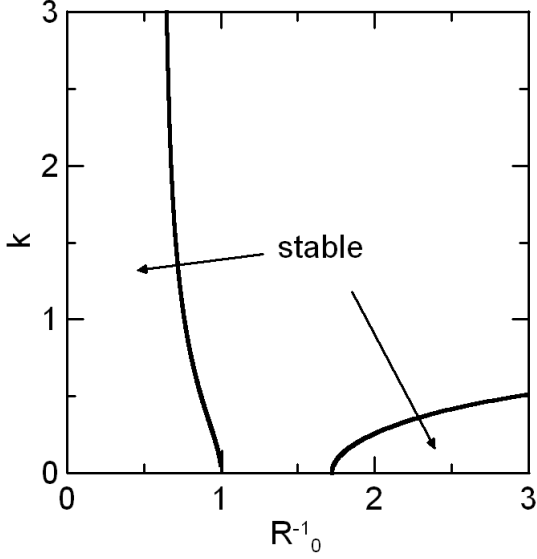


FIG. 7: The phase diagram of the stability in the LL theory as a function of k and R_0 . There are two stable regions.

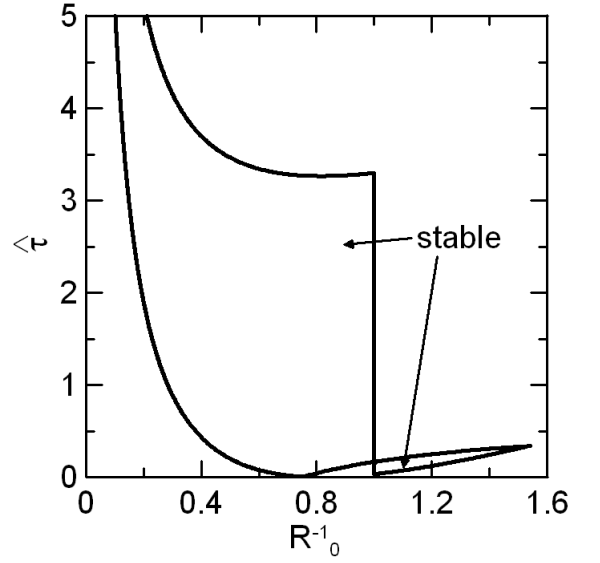


FIG. 8: The phase diagram of the stability in the CD hydrodynamics as a function of $\hat{\tau}$ and R_0 . We set $k = 0$ and $b = 6$. There are two stable regions. Even though $R_0 \geq 1$, the scaling solution of the CD hydrodynamics can be unstable.

Note that we consider the ideal gas equation of state where $\alpha = 1/3$ and $(\partial\sqrt{\alpha}/\partial\phi)_0 = 0$.

One can see that the scaling solution is *unstable* when $\hat{\tau} > 1/b$, for $k = 0$ and $R_0^{-1} = 1 + \epsilon$, and $\hat{\tau} < 1/b$, for $k = 0$ and $R_0^{-1} = 1 - \epsilon$, because the equation for $\delta\theta$ becomes decoupled and A_{22} becomes positive. Here ϵ is a small arbitrary constant.

In general, the analysis of the stability is non-trivial unless the matrix A can be diagonalized. We discuss the stability in the Lyapunov direct method used in [18]. In this approach, the stability of the theory is analyzed by introducing the Lyapunov function, which characterizes the deviation from the scaling solution. The Lyapunov function should be 1) positive definite and 2) monotonically decreasing function with respect to the measure of the distance of the perturbed solution from the non-perturbed one. If we can find the Lyapunov function at given k , b , $\hat{\tau}$ and R_0 , the scaling solution is stable for the parameter set. If the assumed Lyapunov function is found to be a monotonically increasing function then the scaling solution is unstable for the respective parameter set. See Appendix C for details.

However, we should be noted that the stable region predicted in the Lyapunov direct method is normally underestimated, unless we exhaust every possible Lyapunov functions. As an example, let us consider the limit of the LL theory which is realized when we set $\tau_R = \partial \ln \tau_R / \partial \phi = 0$, in Eqs. (57), (58) and (59). In Fig. 7, we show the phase diagram for the stability, on the $k - R_0^{-1}$ plane, assuming the Lyapunov function $V = |\delta\phi|^2 + |\delta\theta|^2$. There are two stable regions; one is in $R_0 \geq 1$ and the other in the small k and small R_0 . We found that the scaling solution is stable also on the line of $R_0 = 1$ by solving the same V , but it is not shown in the phase diagram for simplicity. To confirm more precisely the stable regions, we have to study various possible Lyapunov functions. Then the real stable regions, in general, can distribute in broader regions on the phase diagram. As a matter of fact, the phase diagram obtained by Kouno et al. shows that the LL theory is stable for any k in all region of $R_0 \geq 1$ [18]. On the other hand, we could not find unstable regions for this Lyapunov function. The stability of the domain between the two stable regions is not confirmed. However, from the analysis of Kouno et al., a part of the unconfirmed region should be an unstable region [18].

To analyze the CD hydrodynamics, we first consider the following Lyapunov function V ,

$$V = X^\dagger X = (\delta\phi)^2 + (\delta\theta)^2 + (\delta \ln \Pi)^2. \quad (68)$$

Note that the time evolution of V is given by,

$$\tau \partial_\tau V = X^\dagger (A^\dagger + A) X. \quad (69)$$

For $R_0 = 1$, we can eliminate the variable $\delta\phi$ from the equations. In this case, we will consider the simpler Lyapunov function,

$$V = Y^\dagger Y = (\delta\phi)^2 + (\delta \ln \Pi)^2. \quad (70)$$

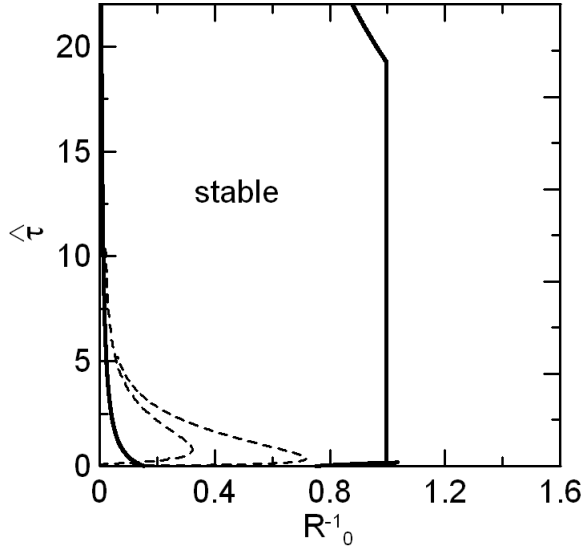


FIG. 9: The phase diagram of the stability in the CD hydrodynamics which is calculated with the Lyapunov function V''' . We set $k = 0$ and $b = 6$. Compared to Fig. (8), the stable region is enlarged.

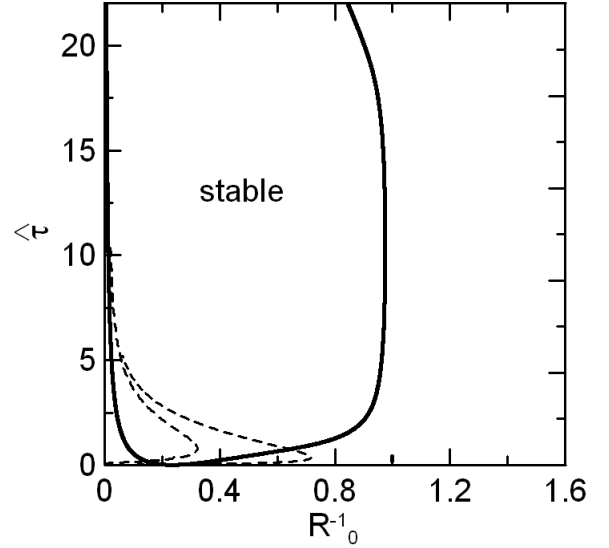


FIG. 10: The phase diagram of the stability in the CD hydrodynamics which is calculated with the Lyapunov function V''' . We set $k = 1$ and $b = 6$. The stable region for homogeneous perturbation ($k = 0$) at low $\hat{\tau}$ around $R_0 = 1$ is changed to the unconfirmed region for the inhomogeneous perturbation ($k = 1$).

Here the evolution equation of Y is given by

$$\tau \partial_\tau Y = BY, \quad (71)$$

where

$$Y = \begin{pmatrix} \delta\phi \\ \delta \ln \Pi \end{pmatrix}, \quad (72)$$

and

$$B = \begin{pmatrix} -(1 + \alpha) & \sqrt{\alpha} \\ -\sqrt{\alpha} \left(\hat{\tau} - \frac{1}{b} \right) + \frac{1}{\sqrt{\alpha b}} + \frac{\sqrt{\alpha} k^2}{b\hat{\tau}-1} & -\frac{1}{b} - \frac{k^2}{b\hat{\tau}-1} \end{pmatrix}. \quad (73)$$

In this case, we should discuss the eigen values of $B^\dagger + B$.

There are three parameters, k , $\hat{\tau}$ and R_0 , fixing $b = 6$. First, we discuss the homogeneous perturbation setting $k = 0$ and calculate the phase diagram in the $\hat{\tau} - R_0^{-1}$ plane, as is shown in Fig. 8. There are two stable regions; one is very small and located in $R_0 < 1$, and the other is larger and located in $R_0 \geq 1$. This result is consistent with the instability of the scaling solution in $\hat{\tau} > 1/b$ for $R_0^{-1} = 1 + \epsilon$ and $\hat{\tau} < 1/b$ for $R_0^{-1} = 1 - \epsilon$. It should, however, be noted that one can see that the scaling solution is always stable on $R_0^{-1} = 0$, which can be seen from the behavior of Eq. (62) itself. On the other hand, we could not find unstable regions. As a matter of fact, we will discuss the stability by using various Lyapunov functions in the following, but still cannot find any unstable regions.

As we have pointed out, the Lyapunov direct method normally underestimates the stable region. To fix the stable region, we have to discuss as many Lyapunov functions as possible. In this work, we analyzed the phase diagram with more three different functions: $V' = |\delta \ln s|^2 + |\delta\theta|^2 + |\delta \ln \Pi|^2$, $V'' = |\delta \ln s|^2 + |\delta\theta|^2 + |R_0^{-1} \delta \ln \Pi|^2$ and $V''' = |\delta\phi|^2 + |\delta\theta|^2 + |R_0^{-1} \delta \ln \Pi|^2$. We found that the qualitative structure of the phase diagram is independent of the choice of these functions. We show the result of V''' in Fig. 9, for which we obtained the maximum stable region (See Appendix D for detailed form of the equation). This phase diagram shows that most part of the phase diagram in $R_0 < 1$ still belongs to the unconfirmed region. As for the region of $R_0 \geq 1$, we found that the stable region strongly depends on the choice of the Lyapunov function, and most of the physically accessible region is confirmed to be stable. As a matter of fact, the dashed lines in Fig. 9 shows the trajectories of the scaling solutions for $a = 0.1$ (left) and $a = 1$ (right), and one can see that most of the trajectories belongs to the stable region in the phase diagram.

In this sense, we conclude that the scaling solution is stable for homogeneous perturbation. To see the stability for the inhomogeneous perturbation, we need to discuss the phase diagram for finite k . In Fig. 10, we show the phase

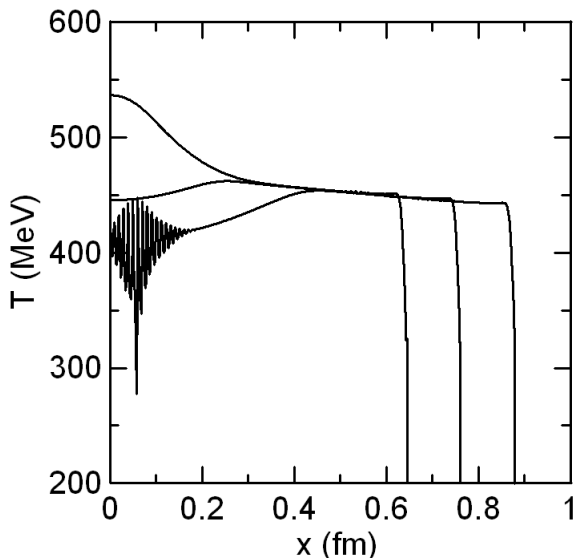


FIG. 11: The numerical simulation of the 1+1 dimensional CD hydrodynamics with $a = 1$ for $t = 0.52$ 0.72 and 0.92 fm. The non-periodic oscillations appear in the center of the fluid.

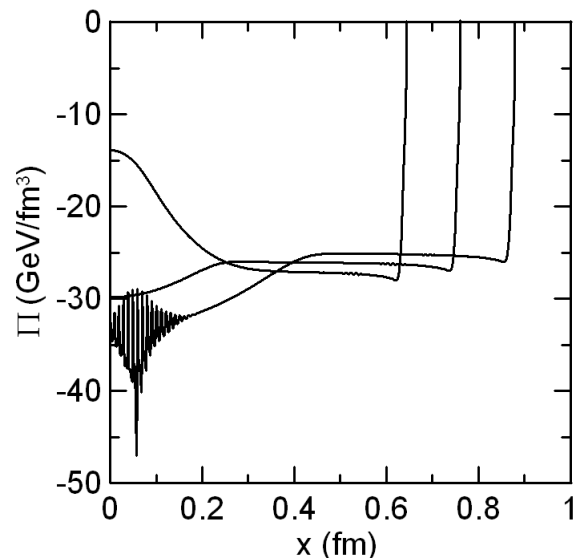


FIG. 12: The numerical simulation of the 1+1 dimensional CD hydrodynamics with $a = 1$ for $t = 0.52$ 0.72 and 0.92 fm. The non-periodic oscillations appear in the center of the fluid.

diagram for $k = 1$, which is calculated by using the function V''' . One can see that the stable region in the low $\hat{\tau}$, near $R_0 = 1$, is changed into a unconfirmed region. This behavior is commonly seen in the results obtained using other three Lyapunov functions. As k increases, this propensity becomes prominent and the stable region shrinks increasingly. The trajectories of the scaling solution are plotted in the same figure, again. One can see that the trajectory of the scaling solution with $a = 1$ passes the unconfirmed region, although the trajectory with $a = 0.1$ still stays inside the stable region. It should be noted that, for $k = 0$, at least a part of the unconfirmed region near $R_0 = 1$ should be unstable. This suggests that the scaling solution can become more unstable for the inhomogeneous perturbation as the bulk viscosity a increases.

The situation discussed here seems to be realized in the numerical simulations of the 1+1 dimensional CD hydrodynamics. When we increase the bulk viscosity a , we found that the numerical calculation becomes unstable and a kind of non-periodic oscillation appears in the center of the fluid. In Figs. 11 and 12, we show the temperature and the bulk viscosity of the viscous fluid with $a = 1$ for $t = 0.52$ 0.72 and 0.92 fm, respectively. We used the Landau initial condition with the initial temperature $T = 590$ MeV and the initial size 0.7 fm. To remove numerical oscillations which will disappear in the continuous limit, we used the additional viscosity which is introduced in [4]. It seems that the oscillation appears when R_0^{-1} exceeds a critical value by decreasing the temperature and the bulk viscosity. The amplitude of the oscillation grows up with time and finally the numerical calculation collapses.

So far, we discussed fixing the parameter $b = 6$ which is consistent with causality. Even when we use the acausal parameter set, $b = 1$, quantitative behavior of the phase diagram is not changed, but the stable region becomes much smaller.

V. CONCLUDING REMARKS

Although the physical importance is recognized for the application in QGP physics, the relativistic viscous hydrodynamics is not well established yet. Some authors use the first order theory to estimate the effect of viscosity in collective observables such as v_2 hoping that the deviation from the ideal hydrodynamics is small so that the theory is of the first order or the second order might be irrelevant. However, the difference between them might be fatal when any instabilities or singularities emerge, such as shock wave propagations. Therefore, it is fundamental to understand the stability of these theories. In this paper, we discussed the causality and stability of the two cases of relativistic dissipative hydrodynamics, the LL theory and CD hydrodynamics.

	LL theory (acausal)	CD hydrodynamics (acausal)	CD hydrodynamics (causal)
hydrostatic state	stable	stable	stable
moving frame	unstable	unstable	stable
scaling solution	stable/unstable	stable/unstable	stable/unstable

The LL theory is known to be acausal whereas the CD hydrodynamics can be causal depending on the values of parameters of the theory. The stability of the theories are summarized in the above Table. Around the hydrostatic state, the LL theory and the CD hydrodynamics are stable. However, when we move to a Lorentz boosted frame, the acausal theories like the LL theory and the CD hydrodynamics with acausal parameter set become unstable. The second line shows that causality and stability are intimately correlated in relativistic dissipative hydrodynamics. The stability of a theory should not depend on the choice of frames. In this sense, the LL theory and the CD hydrodynamics with acausal parameter sets are inconsistent.

The stability of the scaling solution was analyzed by using the Lyapunov direct method. In the LL theory, it is known that the scaling solution is stable against homogeneous and inhomogeneous perturbations when we use initial conditions which satisfies $R_0 \geq 1$ [18]. In the CD hydrodynamics, we found that the scaling solution cannot be stable even for $R_0 \geq 1$. For the homogeneous perturbation ($k = 0$), we confirmed that most parts of the trajectories of the scaling solutions pass the stable region in the phase diagram, which was plotted in terms of $\hat{\tau}$ and R_0^{-1} . Thus, the scaling solution will be stable for the homogeneous perturbation. However, as the k increases, the confirmed stable region in the phase diagram shrinks and the trajectories of the scaling solutions start to penetrate the unconfirmed region. When the unconfirmed regions are real unstable regions, it means that the scaling solution is unstable for inhomogeneous perturbations. This instability is distinguished for larger bulk viscosity because the trajectory with larger viscosity is easier to penetrate the unstable region.

Above conclusion may be supported by the numerical calculations. As a matter of fact, we found that the numerical calculations of the 1+1 dimensional CD hydrodynamics becomes unstable as the bulk viscosity coefficient increases and a kind of non-periodic oscillations appears in the central rapidity region. To see the quantitative signature of the oscillations, we have to investigate various cases with different parameters and initial conditions. This oscillation may be interpreted as turbulence because the instability of the scaling solution indicates chaos which acts as the trigger of turbulence. However, in this work, we could not confirm the unstable region on the phase diagram. To see the appearance of turbulence, we need more systematic study of the instability around the scaling solution beyond the Lyapunov direct method. This is a challenge for the future.

When we discuss the shear viscosity, we have to find the parameters which is consistent with causality as was discussed in this paper. This is also a future task.

T. Koide acknowledges helpful discussions and comments with H. Kouno, I. Mishustin, F. Takagi and G. Torrieri. This work is supported by CNPq and FAPERJ.

APPENDIX A: NON-LINEAR EFFECT FOR CAUSALITY

The propagation speed of the fluid has been discussed based on the linear analysis, and hence the effect of nonlinearity is ignored. In this section, following the discussion of [16, 17], we derive the effect of the nonlinearity in the propagation speed.

For the simple 1+1 dimensional system, the hydrodynamic equations are summarized as follows;

$$(A_\nu^\mu)^t \partial_t Y^\nu + (A_\nu^\mu)^x \partial_x Y^\nu + B^\mu = 0, \quad (\text{A1})$$

where $Y^\mu = (\varepsilon, \theta, \Pi)$ and

$$(A)^t = \begin{pmatrix} \cosh^2 \theta + (\cosh^2 \theta - 1)\alpha & 2w \cosh \theta \sinh \theta & \sinh^2 \theta \\ \cosh \theta \sinh \theta (1 + \alpha) & w(\cosh^2 \theta + \sinh^2 \theta) & \cosh \theta \sinh \theta \\ 0 & \zeta \sinh \theta & \tau_R \cosh \theta \end{pmatrix}, \quad (\text{A2})$$

$$(A)^x = \begin{pmatrix} \cosh \theta \sinh \theta (1 + \alpha) & w(\cosh^2 \theta + \sinh^2 \theta) & \cosh \theta \sinh \theta \\ \sinh^2 \theta + (\sinh^2 \theta + 1)\alpha & 2w \cosh \theta \sinh \theta & \cosh^2 \theta \\ 0 & \zeta \cosh \theta & \tau_R \sinh \theta \end{pmatrix}, \quad (\text{A3})$$

$$B^\mu = (0, 0, 0, \Pi). \quad (\text{A4})$$

Here, w is the effective enthalpy density, $w = \varepsilon + P + \Pi$.

The characteristic speed v is given by

$$\det(v(A)^t - (A)^x) = 0. \quad (\text{A5})$$

The speed is easily estimated in the local rest frame, $\theta = 0$. Then we have the following three solutions,

$$v = 0, \pm \sqrt{\frac{\alpha w \tau_R + \zeta}{w \tau_R}}. \quad (\text{A6})$$

One can easily see that if Π is small and we can replace w with $\varepsilon + P$, this result is same as Eq. (19).

We consider the case of the effective enthalpy density is positive. Then, to satisfy causality, the transport coefficients should satisfy the following condition,

$$\frac{\zeta}{\tau_R} \leq (1 - \alpha)(\varepsilon + P + \Pi). \quad (\text{A7})$$

This is, again, the generalization of the restriction for the transport coefficients discussed below Eq. (6).

APPENDIX B: INSTABILITY IN GENERAL EQUILIBRIUM FRAME (HISCOCK-LINDBLAM)

In section , the stability from a Lorentz boosted frame was discussed. A similar problem was discussed by Hiscock and Lindblam [14]. In this appendix, we apply their discussion to the CD hydrodynamics.

They consider the transformation of the coordinate by using the following replacement of the variables,

$$\omega = \gamma(\tilde{\omega} + v\tilde{k}), \quad (\text{B1})$$

$$k = \gamma(\tilde{k} + v\tilde{\omega}), \quad (\text{B2})$$

where ω and k are variables in the rest frame, and $\tilde{\omega}$ and \tilde{k} are in the new frame, which moves with the velocity v . Substituting into the result obtained in the rest frame (16), we have

$$\gamma^3(\tilde{\omega} + v\tilde{k})^3 - \frac{i}{\tau_R}\gamma^2(\tilde{\omega} + v\tilde{k})^2 - \left(\frac{\zeta}{\tau_R}\frac{1}{\varepsilon + P} + \alpha\right)\gamma^3(\tilde{k} + v\tilde{\omega})^2(\tilde{\omega} + v\tilde{k}) + i\frac{\alpha}{\tau_R}\gamma^2(\tilde{k} + v\tilde{\omega})^2 = 0. \quad (\text{B3})$$

We can easily solve the equation for $\tilde{k} = 0$,

$$\tilde{\omega} = 0, 0, \frac{i}{\tau_R} \frac{1 - \alpha v^2}{\gamma(1 - \frac{\zeta}{\tau_R} \frac{v^2}{\varepsilon + P} - \alpha v^2)}. \quad (\text{B4})$$

The imaginary part is positive and hence the theory is still stable.

On the other hand, in the LL theory, the solutions are given by

$$\tilde{\omega} = 0, 0, -i \frac{(\varepsilon + P)(1 - \alpha v^2)}{\zeta \gamma v^2}. \quad (\text{B5})$$

Thus, the LL theory is unstable again.

APPENDIX C: LYAPUNOV DIRECT METHOD

Here, we summarize the stability analysis based on the Lyapunov function. As an example, let us consider the damped harmonic oscillator,

$$\frac{\partial}{\partial t} x = v, \quad (\text{C1})$$

$$\frac{\partial}{\partial t} v = -\gamma v - \omega^2 x. \quad (\text{C2})$$

The solution of the equation converges to $x = v = 0$.

To discuss the stability around the equilibrium solution $x_0 = v_0 = 0$, we introduce a function which characterizes the deviation from the equilibrium. For example, we choose

$$V = (v - v_0)^2 + \alpha^2(x - x_0)^2. \quad (\text{C3})$$

This is positive definite and if this function monotonically decreases with time, the system is stable and the function V is called the Lyapunov function. The time evolution of the function V is given by

$$\frac{d}{dt}V = (\alpha(x - x_0), v - v_0)M \begin{pmatrix} \alpha(x - x_0) \\ v - v_0 \end{pmatrix}, \quad (\text{C4})$$

where

$$M = \begin{pmatrix} 0 & \alpha - \frac{\omega^2}{\alpha} \\ \alpha - \frac{\omega^2}{\alpha} & -2\gamma \end{pmatrix}. \quad (\text{C5})$$

The eigen values of the matrix M are given by

$$\lambda_{\pm} = \frac{1}{2}(-\gamma \pm \sqrt{\gamma^2 + (\alpha - \omega^2/\alpha)^2}). \quad (\text{C6})$$

One can see that when $\alpha = \omega$, V is a monotonically decreasing function in time. Thus V is the Lyapunov function and the equilibrium state is stable.

However, if we use $\alpha \neq \omega$, the function generally have a positive and negative eigen values. Thus we cannot determine the stability of the equilibrium solution. In this sense, the Lyapunov direct method usually underestimates the stability of the system.

Similarly, when we find that the minimum eigen value is positive and hence V is a monotonically increasing function, the equilibrium solution is unstable.

APPENDIX D: ANOTHER CASE OF THE FUNCTION V'''

Instead of Eq. (63), we introduce the following vector,

$$X = \begin{pmatrix} \delta\phi \\ \delta\theta \\ R_0^{-1}\delta \ln \Pi \end{pmatrix}. \quad (\text{D1})$$

Then, the Lyapunov function is given by

$$V''' = X^\dagger X = |\delta\phi|^2 + |\delta\theta|^2 + (R_0^{-1})^2 |\delta \ln \Pi|^2. \quad (\text{D2})$$

Then the evolution equation of the Lyapunov function is

$$\tau \partial_\tau V''' = X^\dagger (A^\dagger + A) X, \quad (\text{D3})$$

where

$$A = \begin{pmatrix} -(1 - R_0^{-1}) \left(\frac{\partial \sqrt{\alpha}}{\partial \phi} \right)_0 - R_0^{-1} (1 + \alpha) & -(1 - R_0^{-1}) \sqrt{\alpha} (-ik) & \sqrt{\alpha} \\ -\sqrt{\alpha} \frac{(-ik)}{(1 - R_0^{-1})} & -(1 - \alpha) - \frac{(R_0^{-1} \hat{\tau} - \frac{1}{b})}{(1 - R_0^{-1})} & \frac{(-ik)}{(1 - R_0^{-1})} \\ -\sqrt{\alpha} \left(R_0^{-1} \hat{\tau} - \frac{1}{b} \right) + \frac{1}{\sqrt{\alpha b}} & \frac{-ik}{b} & -\hat{\tau} - (1 - R_0^{-1})(1 + \alpha) \end{pmatrix}. \quad (\text{D4})$$

Similarly, as for $R_0 = 1$, the matrix B is given by

$$B = \begin{pmatrix} -(1 + \alpha) & \sqrt{\alpha} \\ -\sqrt{\alpha} \left(\hat{\tau} - \frac{1}{b} \right) + \frac{1}{\sqrt{\alpha b}} + \frac{\sqrt{\alpha} k^2}{b\hat{\tau} - 1} & -\hat{\tau} - \frac{k^2}{b\hat{\tau} - 1} \end{pmatrix}. \quad (\text{D5})$$

[1] See for example, Hama Y, Kodama T and Socolowski Jr O 2005 Braz. J. Phys. **35** 24; Huovinen P and Ruuskanen P V 2006 Ann. Rev. Nucl. Part. Sci. **56** 163; Ollitrault J Y 2008 Euro. J. Phys. **29**, 275 and references therein.

- [2] Danielewicz P and Gyulassy M 1985 Phys. Rev. **D31** 53; Teany D 2003 Phys. Rev. **C68** 034913; Van P, Biro T S 2008 Eur. Phys. J. ST **155** 201; Muronga A 2002 Phys. Rev. Lett. **88** 062302 [Erratum ibid. 2002 **89** 159901]; 2007 Phys. Rev. **C76** 014909; Romatschke P and Romatschke U 2007 Phys. Rev. Lett. **99** 172301; Song H and Heinz U W, arXiv:0712.3715; Chaudhuri A K, arXiv:0801.3180; Dusling K and Teaney D, arXiv:0710.5932; Bhalerao R S and Gupta S 2008 Phys. Rev. **C77** 014902 ; Dumitru A Molnár E and Nara Y 2007 Phys. Rev. **C76**, 024910 ; Pratt S 2008 Phys. Rev. **C77**, 024910; Molnar D and Huovinen P, arXiv:0806.1367; Molnár E, arXiv:0807.0544 and references therein.
- [3] Koide T, Denicol G S, Mota Ph and Kodama T 2007 Phys. Rev. **C75** 034909
- [4] Denicol G S, Kodama T, Koide T and Mota Ph, arXiv:0805.1719
- [5] Landau L D and Lifshitz E M, *Fluid Mechanics*, (Pergamon; Addison-Wesley, London, U.K.; Reading, U.S.A., 1959)
- [6] Eckart C 1940 Phys. Rev. **58** 919
- [7] Israel W 1976 Ann. Phys. (N.Y.) **100** 310; Israel W and Stewart J M 1979 Proc. R. Soc. Lond. A **357** 43; Israel W and Stewart J M 1979 Ann. Phys. (N.Y.) **118** 341
- [8] Jou D, Casas-Vázquez J, and Lebon G 1988 Rep. Prog. Phys. **51** 1105; 1999 **62** 1035
- [9] Müller I 1967 Z. Phys. **198** 329; Müller I and Ruggeri T 1986 Ann. Phys. (N.Y.) **169** 191; as a review paper, see Müller I 1999 Living Rev. Relativ. **2** 1
- [10] Carter B 1991 Proc. R. Soc. London, Ser A, **433**, 45; as a review paper, see Andersson N and Comer G L 2007 Living Rev. Relativity **10**, 1
- [11] Grmela M and Öttinger H C 1997 Phys. Rev. **E56**, 6620
- [12] Hiscock W A and Lindblom L 1983 Ann. Phys. (N.Y.), **151** 466
- [13] Hiscock W A and Lindblom L 1985 Phys. Rev. **D31** 725
- [14] Hiscock W A and Lindblom L 1987 Phys. Rev. **D35** 3723
- [15] Hiscock W A and Lindblom L 1988 Phys. Lett. **A131** 509
- [16] Hiscock W A and Lindblom L 1988 Phys. Lett. **A 131** 509
- [17] Hiscock W A and Olson T S 1989 Phys. Lett. **A141** 125
- [18] Kouno H, Maruyama M, Takagi F and Saito K 1990 Phys. Rev. **D41** 2903
- [19] Torrieri G and Mishustin I, arXiv:0805.0442
- [20] It is noteworthy that the transport coefficients of the CD hydrodynamics cannot be estimated by using the Green-Kubo-Nakano formula. See the following references; Koide T 2007 Phys. Rev. **E75** 060103(R); Koide T and Kodama T, arXiv:0806.3725.